11

Mobile Robots

Solution to Problem 11.1

Denote by (x, y) the Cartesian coordinates of a representative point on the tricycle (e.g., the midpoint of the rear wheel axle), by ϕ the steering angle of the front wheel with respect to the vehicle, and by θ_0 the orientation of the vehicle with respect to the x axis. Once the configuration of the tricycle and of the first $i-1$ trailers are given, the configuration of the i-th trailer is completely described by the its orientation θ_i with respect to the x axis. The configuration vector for the complete vehicle is therefore obtained as $\boldsymbol{q} = [\, x \quad y \quad \phi \quad \theta_0 \quad \theta_1 \quad \dots \quad \theta_N \,]^T$, and takes values in $\mathbb{R}^2 \times SO(2) \times \ldots \times SO(2)$ (with $SO(2)$ appearing $N+2$ times). Another possibility is to replace the absolute angle θ_i with the relative angle $\theta_i - \theta_{i-1}$ to describe the orientation of each trailer.

Solution to Problem 11.2

Add the kinematic constraints side-by-side to obtain

$$3\,\ell\,\dot{q}_3 + r(\dot{q}_4 + \dot{q}_5 + \dot{q}_6) = 0$$

that can be integrated as

$$q_3 = -\frac{r}{3\,\ell}\,(q_4 + q_5 + q_6) + c,$$

where c is an integration constant. The kinematic constraints are then partially integrable. In particular, the orientation q_3 of the robot is a linear function of the wheel rotation angles q_4, q_5, q_6.

Solution to Problem 11.3

Consider a single Pfaffian constraint

$$\boldsymbol{a}^T(\boldsymbol{q})\dot{\boldsymbol{q}} = \sum_{j=1}^{n} a_j(\boldsymbol{q})\dot{q}_j = 0.$$

The corresponding kinematic model is

$$\dot{\boldsymbol{q}} = \sum_{j=1}^{n-1} \boldsymbol{g}_j(\boldsymbol{q}) u_j,$$

where $\{\boldsymbol{g}_1(\boldsymbol{q}), \ldots, \boldsymbol{g}_{n-1}(\boldsymbol{q})\}$ is a basis of $\mathcal{N}(\boldsymbol{a}^T(\boldsymbol{q}))$. Without loss of generality, assume that $a_1(\boldsymbol{q}) \neq 0$, and consider the following choice of input vector fields

$$\boldsymbol{g}_1 = \begin{bmatrix} -\gamma(\boldsymbol{q})a_2(\boldsymbol{q}) \\ \gamma(\boldsymbol{q})a_1(\boldsymbol{q}) \\ 0 \\ 0 \\ \vdots \\ 0 \\ 0 \end{bmatrix} \quad \boldsymbol{g}_2 = \begin{bmatrix} -\gamma(\boldsymbol{q})a_3(\boldsymbol{q}) \\ 0 \\ \gamma(\boldsymbol{q})a_1(\boldsymbol{q}) \\ 0 \\ \vdots \\ 0 \\ 0 \end{bmatrix} \quad \cdots \quad \boldsymbol{g}_{n-1} = \begin{bmatrix} -\gamma(\boldsymbol{q})a_n(\boldsymbol{q}) \\ 0 \\ 0 \\ 0 \\ \vdots \\ 0 \\ \gamma(\boldsymbol{q})a_1(\boldsymbol{q}) \end{bmatrix}$$

where $\gamma(\boldsymbol{q}) \neq 0$. The distribution $\Delta = \text{span}\{\boldsymbol{g}_1, \ldots, \boldsymbol{g}_{n-1}\}$ is involutive if any Lie bracket $[\boldsymbol{g}_i, \boldsymbol{g}_j]$ can be written as a linear combination of $\boldsymbol{g}_1, \ldots, \boldsymbol{g}_{n-1}$.

For example, consider $[\boldsymbol{g}_1, \boldsymbol{g}_2]$. A simple computation gives

$$[\boldsymbol{g}_1, \boldsymbol{g}_2] = \begin{bmatrix} \dfrac{\partial(\gamma a_2)}{\partial q_1}\gamma a_3 - \dfrac{\partial(\gamma a_3)}{\partial q_1}\gamma a_2 + \left(\dfrac{\partial(\gamma a_3)}{\partial q_2} - \dfrac{\partial(\gamma a_2)}{\partial q_3}\right)\gamma a_1 \\ \dfrac{\partial(\gamma a_1)}{\partial q_3}\gamma a_1 - \dfrac{\partial(\gamma a_1)}{\partial q_1}\gamma a_3 \\ \dfrac{\partial(\gamma a_1)}{\partial q_1}\gamma a_2 - \dfrac{\partial(\gamma a_1)}{\partial q_2}\gamma a_1 \\ 0 \\ \vdots \\ 0 \end{bmatrix}$$

Using the integrability condition expressed by (11.9), one easily verifies that

$$[\boldsymbol{g}_1, \boldsymbol{g}_2] = \frac{\partial(\gamma a_3)}{\partial q_1}\boldsymbol{g}_1 - \frac{\partial(\gamma a_2)}{\partial q_1}\boldsymbol{g}_2 + \frac{\partial(\gamma a_1)}{\partial q_1}\frac{a_3\boldsymbol{g}_1 + a_2\boldsymbol{g}_2}{a_1},$$

i.e., $[\boldsymbol{g}_1, \boldsymbol{g}_2]$ is a linear combination of $\boldsymbol{g}_1$, $\boldsymbol{g}_2$.

A similar construction can be repeated for any Lie bracket $[\boldsymbol{g}_i, \boldsymbol{g}_j]$; hence, the distribution Δ is involutive under the integrability condition (11.9).

Solution to Problem 11.4

Consider a set of k Pfaffian constraints

$$\boldsymbol{A}^T\dot{\boldsymbol{q}} = \boldsymbol{0}$$

with a constant constraint matrix $\boldsymbol{A}^T$. Then, the associated kinematic model

$$\dot{\boldsymbol{q}} = \sum_{j=1}^{m} \boldsymbol{g}_j u_j = \boldsymbol{G}\,\boldsymbol{u} \qquad m = n - k \tag{S11.1}$$

has constant input vector fields $\boldsymbol{g}_1, \ldots, \boldsymbol{g}_m$. Its accessibility distribution $\Delta_{\mathcal{A}}$ is clearly involutive, because $[\boldsymbol{g}_i, \boldsymbol{g}_j] = 0$ for any i, j. The controllability condition (11.11) is hence violated, and in particular

$$\dim \Delta_{\mathcal{A}}(\boldsymbol{q}) = m.$$

Therefore, the above set of Pfaffian constraints is completely integrable, i.e., holonomic. This obvious conclusion could have also been reached by noting that (S11.1) is in fact a driftless linear system, and using directly the controllability rank condition (D.15).

Solution to Problem 11.5

Integration of the kinematic model (11.13) under the given input sequence starting from the initial configuration $\boldsymbol{q}_0 = [\, x_0 \quad y_0 \quad \theta_0 \,]^T$ provides

$$\begin{aligned} x(4\varepsilon) &= x_0 + \varepsilon \cos\theta_0 - \varepsilon \cos(\theta_0 + \varepsilon) \\ y(4\varepsilon) &= y_0 + \varepsilon \sin\theta_0 - \varepsilon \sin(\theta_0 + \varepsilon) \\ \theta(4\varepsilon) &= \theta_0. \end{aligned}$$

The displacement is therefore

$$\boldsymbol{q}(4\varepsilon) - \boldsymbol{q}_0 = \begin{bmatrix} \varepsilon \cos\theta_0 - \varepsilon \cos(\theta_0 + \varepsilon) \\ \varepsilon \sin\theta_0 - \varepsilon \sin(\theta_0 + \varepsilon) \\ 0 \end{bmatrix} = \varepsilon^2\, \boldsymbol{t},$$

with

$$\boldsymbol{t} = \begin{bmatrix} \dfrac{\cos\theta_0 - \cos(\theta_0 + \varepsilon)}{\varepsilon} \\ \dfrac{\sin\theta_0 - \sin(\theta_0 + \varepsilon)}{\varepsilon} \\ 0 \end{bmatrix}$$

— compare with the expression of the displacement for a generic two-input system as given in Appendix D.

Finally, one obtains

$$\lim_{\varepsilon \to 0} \boldsymbol{t} = \begin{bmatrix} -\left.\dfrac{d\cos\theta}{d\theta}\right|_{\theta=\theta_0} \\ -\left.\dfrac{d\sin\theta}{d\theta}\right|_{\theta=\theta_0} \\ 0 \end{bmatrix} = \begin{bmatrix} \sin\theta_0 \\ -\cos\theta_0 \\ 0 \end{bmatrix},$$

that coincides with the value at $\boldsymbol{q}_0$ of the Lie Bracket of the two input vector fields (see Sect. 11.2.1).

Solution to Problem 11.6

With reference to Figs. 1.13 and 11.3, denote by $\boldsymbol{p}_R = [\,x_R \quad y_R\,]^T$, $\boldsymbol{p}_L = [\,x_L \quad y_L\,]^T$ and $\boldsymbol{p}_M = [\,x_M \quad y_M\,]^T$ respectively the position vector of the right wheel centre, of the left wheel centre and of the midpoint between the two. Since

$$\begin{aligned}\dot{x}_i &= r\,\omega_i \cos\theta \\ \dot{y}_i &= r\,\omega_i \sin\theta,\end{aligned}$$

where $i = R, L$, one obtains

$$\begin{aligned}\dot{x}_M &= \frac{\dot{x}_R + \dot{x}_L}{2} = r\cos\theta\,\frac{\omega_R + \omega_L}{2} \\ \dot{y}_M &= \frac{\dot{y}_R + \dot{y}_L}{2} = r\sin\theta\,\frac{\omega_R + \omega_L}{2}\end{aligned}$$

and therefore

$$v = \sqrt{\dot{x}_M^2 + \dot{y}_M^2} = \frac{r\,(\omega_R + \omega_L)}{2}.$$

The expression of the angular velocity of the robot can be obtained by applying the general velocity composition rule (B.4) and making use of the skew-symmetric operator $\boldsymbol{S}(\cdot)$:

$$\dot{\boldsymbol{p}}_R = \dot{\boldsymbol{p}}_L + \boldsymbol{S}(\omega)(\boldsymbol{p}_R - \boldsymbol{p}_L), \tag{S11.2}$$

where

$$\boldsymbol{S}(\omega) = \begin{bmatrix} 0 & -\omega \\ \omega & 0 \end{bmatrix}$$

because the motion of the robot is planar. Using the expressions of $\dot{\boldsymbol{p}}_R$, $\dot{\boldsymbol{p}}_L$ and the fact that

$$\boldsymbol{p}_R = \boldsymbol{p}_L + \begin{bmatrix} d\sin\theta \\ -d\cos\theta \end{bmatrix},$$

Equation (S11.2) becomes

$$\begin{bmatrix} r\,\omega_R\cos\theta \\ r\,\omega_R\sin\theta \end{bmatrix} = \begin{bmatrix} r\,\omega_L\cos\theta \\ r\,\omega_L\sin\theta \end{bmatrix} + \begin{bmatrix} 0 & -\omega \\ \omega & 0 \end{bmatrix} \begin{bmatrix} d\sin\theta \\ -d\cos\theta \end{bmatrix}.$$

Squaring and adding side-by-side these two equations leads to

$$\omega^2 = \frac{r^2(\omega_R - \omega_L)^2}{d^2}.$$

Using again one of the two equations, it can be concluded that the only solution is

$$\omega = \frac{r(\omega_R - \omega_L)}{d}.$$

Solution to Problem 11.7

With reference to Fig. 11.4, denote by (x_C, y_C) the Cartesian coordinates of the instantaneous centre of rotation C in the world reference frame, and by (x'_C, y'_C) its coordinates in a moving frame having the origin at the centre of the rear wheel and the x' axis aligned with the bicycle body. Simple geometry gives

$$\begin{bmatrix} x'_c \\ y'_c \end{bmatrix} = \begin{bmatrix} 0 \\ \ell/\tan\phi \end{bmatrix}$$

and thus

$$\begin{bmatrix} x_c \\ y_c \end{bmatrix} = \begin{bmatrix} x \\ y \end{bmatrix} + \boldsymbol{R}(\theta) \begin{bmatrix} x'_c \\ y'_c \end{bmatrix} = \begin{bmatrix} x - \ell \sin\theta/\tan\phi \\ y + \ell\cos\theta/\tan\phi \end{bmatrix},$$

where

$$\boldsymbol{R}(\theta) = \begin{bmatrix} \cos\theta & -\sin\theta \\ \sin\theta & \cos\theta \end{bmatrix}$$

is the (planar) rotation matrix of the moving frame with respect to the world frame.

Since the velocity vector of a generic point P on the robot body is tangent to the circle centred at C and passing through P, the modulus of the angular velocity of the bicycle is obtained as

$$\omega_{\text{body}} = v_P / R_P, \tag{S11.3}$$

where v_P is the modulus of the velocity of P, and R_P is its instantaneous radius of rotation (i.e., its radius of curvature):

$$R_P = \sqrt{(x_P - x_C)^2 + (y_P - y_C)^2}.$$

The resulting ω_{body} is obviously the same for any choice of P. In particular, by choosing P as the centre of the rear wheel, one has $R_P = \ell/\tan\phi$, and thus

$$\omega_{\text{body}} = \dot{\theta} = v\tan\phi/\ell,$$

consistently with the evolution of θ predicted by the kinematic model (11.19). Finally, plugging this expression of ω in (S11.3) yields

$$v_P = R_p\, v\tan\phi/\ell.$$

Solution to Problem 11.8

With the configuration vector $\boldsymbol{q} = [\, x \quad y \quad \phi \quad \theta_0 \quad \theta_1 \ldots \theta_N \,]^T$ defined in the solution to Problem 11.1, the $N+2$ kinematic constraints are

$$\begin{aligned} \dot{x}_f \sin(\theta_0 + \phi) - \dot{y}_f \cos(\theta_0 + \phi) &= 0 \\ \dot{x} \sin\theta_0 - \dot{y} \cos\theta_0 &= 0 \\ \dot{x}_i \sin\theta_i - \dot{y}_i \cos\theta_i &= 0 \qquad i = 1, \ldots, N, \end{aligned}$$

where (x_f, y_f) and (x_i, y_i) are the Cartesian coordinates of the centre of the tricycle front wheel and of the i-th trailer wheel axle midpoint, respectively (compare with (11.15), (11.16)). Denote by ℓ the distance between the front wheel and the rear axle of the tricycle, and by ℓ_i the hinge-to-hinge length of the i-th trailer. It is

$$\begin{aligned} x_f &= x + \ell \cos\theta_0 \\ y_f &= y + \ell \sin\theta_0 \end{aligned}$$

and

$$\begin{aligned} x_i &= x - \sum_{j=1}^{i} \ell_j \cos\theta_j \\ y_i &= y - \sum_{j=1}^{i} \ell_j \sin\theta_j, \end{aligned}$$

so that the kinematic constraints become

$$\begin{aligned} \dot{x} \sin(\theta_0 + \phi) - \dot{y} \cos(\theta_0 + \phi) - \dot{\theta}_0 \, \ell \cos\phi &= 0 \\ \dot{x} \sin\theta_0 - \dot{y} \cos\theta_0 &= 0 \\ \dot{x} \sin\theta_i - \dot{y} \cos\theta_i + \sum_{j=1}^{i} \dot{\theta}_j \, \ell_j \cos(\theta_i - \theta_j) &= 0 \quad i = 1, \ldots, N. \end{aligned}$$

The null space of the constraint matrix is spanned by the two columns of

$$G(q) = \begin{bmatrix} \cos\theta_0 & 0 \\ \sin\theta_0 & 0 \\ 0 & 1 \\ \frac{1}{\ell}\tan\phi & 0 \\ -\frac{1}{\ell_1}\sin(\theta_1 - \theta_0) & 0 \\ -\frac{1}{\ell_2}\cos(\theta_1 - \theta_0)\sin(\theta_2 - \theta_1) & 0 \\ \vdots & \vdots \\ -\frac{1}{\ell_i}\left(\prod_{j=1}^{i-1}\cos(\theta_j - \theta_{j-1})\right)\sin(\theta_i - \theta_{i-1}) & 0 \\ \vdots & \vdots \\ -\frac{1}{\ell_N}\left(\prod_{j=1}^{N-1}\cos(\theta_j - \theta_{j-1})\right)\sin(\theta_N - \theta_{N-1}) & 0 \end{bmatrix} = [\, \boldsymbol{g}_1(\boldsymbol{q}) \; \boldsymbol{g}_2(\boldsymbol{q}) \,]$$

(compare with (11.19)). The kinematic control system is then

$$\dot{\boldsymbol{q}} = \boldsymbol{g}_1(\boldsymbol{q})\, v + \boldsymbol{g}_2(\boldsymbol{q})\, \omega,$$

where v and ω are respectively the driving velocity of the rear wheels and the steering velocity of the tricycle.

Solution to Problem 11.9

According to (11.14), the velocity inputs of the equivalent unicycle model are given by

$$\begin{aligned} v &= \frac{r\,(\omega_R + \omega_L)}{2} \\ \omega &= \frac{r\,(\omega_R - \omega_L)}{d}, \end{aligned}$$

where r is the wheel radius and d is the distance between the wheel centres. Solving for ω_R in the first and replacing the obtained expression in the second yields

$$\begin{aligned} \omega_L &= \frac{2v - d\,\omega}{2r} \\ \omega_R &= \frac{2v + d\,\omega}{2r}. \end{aligned}$$

The resulting constraints on v, ω are then

$$\begin{aligned} \left| \frac{2v(t) - d\,\omega(t)}{2r} \right| &\leq \omega_{RL} \\ \left| \frac{2v(t) + d\,\omega(t)}{2r} \right| &\leq \omega_{RL}, \end{aligned}$$

that correspond to a rhombus-shaped admissible region in the v, ω plane. In particular, the maximum achievable values for these velocities are easily computed as the intercepts of the sides of the rhombus with the v, ω axes, i.e., $\pm r\,\omega_{RL}$ for the driving velocity and $\pm 2\,r\,\omega_{RL}/d$ for the steering velocity.

Solution to Problem 11.10

The geometric version of the (2,4) chained form is

$$\begin{aligned} z_1' &= \widetilde{v}_1 \\ z_2' &= \widetilde{v}_2 \\ z_3' &= z_2 \widetilde{v}_1 \\ z_4' &= z_3 \widetilde{v}_1. \end{aligned}$$

Choose the geometric inputs $\widetilde{v}_1$, $\widetilde{v}_2$ in the parameterized form (11.49), with $\Delta = z_{1,f} - z_{1,i}$ and $s \in [s_i, s_f] = [0, |\Delta|]$. Integrating in a recursive fashion the second, third and fourth equations and setting $z_2(s_f) = z_{2,f}$, $z_3(s_f) = z_{3,f}$ and $z_4(s_f) = z_{4,f}$ leads to a linear system in the form (11.50) where

$$\boldsymbol{D} = \begin{bmatrix} |\Delta| & \frac{\Delta^2}{2} & \frac{|\Delta|^3}{3} \\ \mathrm{sgn}(\Delta)\frac{\Delta^2}{2} & \frac{\Delta^3}{6} & \mathrm{sgn}(\Delta)\frac{\Delta^4}{12} \\ \frac{|\Delta|^3}{6} & \frac{\Delta^4}{24} & \frac{|\Delta|^5}{60} \end{bmatrix} \quad \boldsymbol{d} = \begin{bmatrix} z_{2,f} - z_{2,i} \\ z_{3,f} - z_{3,i} - z_{2,i}\Delta \\ z_{4,f} - z_{4,i} - z_{3,i}\Delta - z_{2,i}|\Delta| \end{bmatrix}.$$

Solution to Problem 11.11

It is sufficient to modify (11.48) as follows:

$$\widetilde{v}_1 = \Delta = z_{1,f} - z_{1,i},$$

with the second input (11.49) unchanged. With this choice, z_1 will reach its final desired value exactly at $s_f = 1$. The coefficients $c_0, \ldots, c_{n-2}$ in (11.49) are computed by solving a linear system of equations that is still in the general form (11.50). For example, in the case of the $(2, 3)$ chained form, one obtains

$$\boldsymbol{D} = \begin{bmatrix} 1 & 1/2 \\ \Delta/2 & \Delta/6 \end{bmatrix} \quad \boldsymbol{d} = \begin{bmatrix} z_{2,f} - z_{2,i} \\ z_{3,f} - z_{3,i} - z_{2,i}\Delta \end{bmatrix}.$$

Solution to Problem 11.12

As shown in the solution to Problem 11.11, the path planning scheme based on parameterized inputs (scheme A in the following) must be modified by letting

$$\widetilde{v}_1 = \Delta = z_{1,f} - z_{1,i}$$

to obtain $s_f = 1$ and allow a comparison with the scheme that uses interpolating polynomials of different degree (scheme B in the following). With scheme A one has then

$$z_1(s) = z_{1,i} + (z_{1,f} - z_{1,i})s$$

that coincides with the expression of $z_1(s)$ generated by scheme B. Moreover, being

$$\widetilde{v}_2 = c_0 + c_1 s$$

for a (2,3) chained form, it is

$$z_2(s) = z_{2,i} + c_0\, s + c_1\, s^2/2$$

and

$$z_3(s) = z_{3,i} + \Delta \int_0^s (c_0\, \sigma + c_1\, \sigma^2/2) d\sigma = z_{3,i} + \Delta\, (c_0\, s^2/2 + c_1\, s^3/6).$$

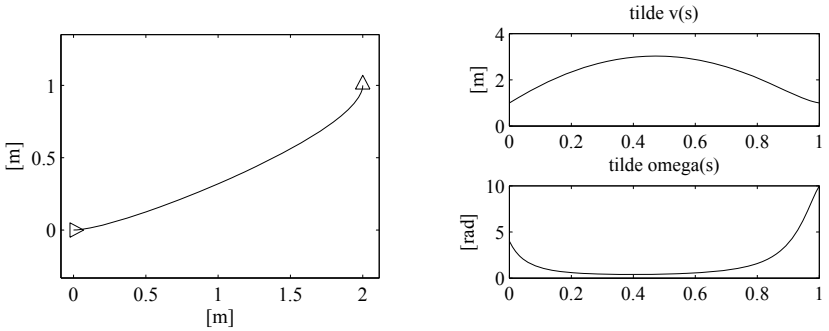

Fig. S11.1. Path planning via Cartesian polynomials; *left*: Cartesian path of the unicycle for the required parking manoeuvre, *right*: geometric inputs along the path

Hence, $z_3(s)$ with scheme A is a cubic polynomial in s, as is with scheme B. However, there is a unique cubic polynomial that meets the two boundary conditions on z_3 and the two boundary conditions on z_2

$$\frac{z_3'(0)}{z_1'(0)} = z_{2i} \qquad \frac{z_3'(1)}{z_1'(1)} = z_{2f}.$$

Hence, the expressions of $z_3(s)$ generated by the two schemes coincide. Since z_1 and z_3 are flat outputs for a (2,3) chained form (see the end of Sect. 11.5.2), a unique $z_2(s)$ is associated to $z_1(s)$ and $z_3(s)$. One can then conclude that the paths in the $\boldsymbol{z}$ space (and the associated geometric inputs) generated by the two schemes are exactly the same.

Solution to Problem 11.13

The files with the solution can be found in Folder `11_13`. For the required manoeuvre, the coefficients of the interpolating polynomials

$$x(s) = s^3 x_f - (s-1)^3 x_i + \alpha_x s^2(s-1) + \beta_x s(s-1)^2$$
$$y(s) = s^3 y_f - (s-1)^3 y_i + \alpha_y s^2(s-1) + \beta_y s(s-1)^2$$

are found to be

$$\alpha_x = -6 \qquad \beta_x = 1$$
$$\alpha_y = -2 \qquad \beta_y = 0$$

where $k_i = k_f = 1$. The corresponding unicycle path is shown in Fig. S11.1.

Using the flatness property of the unicycle, expressed by (11.45), (11.46) and (11.47), File `s11_13.m` also generates the geometric inputs $\widetilde{v}(s)$, $\widetilde{\omega}(s)$ along the path, as shown in Fig. S11.1.

There are several ways to find a feasible timing law $s = s(t)$ over the planned path. For example, one may simply let $s = t$, so that $v(t)$ and $\omega(t)$

coincide with $\widetilde{v}(s)$ and $\widetilde{\omega}(s)$, respectively. However, both the inputs violate the given bounds; in particular, the maximum value is attained by ω at 10 rad/sec. A uniform scaling procedure with $T = 10$ can then be used to slow down the trajectory and recover the feasibility of the inputs (see (11.54), (11.55)).

Solution to Problem 11.14

The (2,3) chained form is

$$\begin{aligned} \dot{z}_1 &= v_1 \\ \dot{z}_2 &= v_2 \\ \dot{z}_3 &= z_2\, v_1. \end{aligned}$$

Assume that a desired state trajectory $(z_{1d}(t), z_{2d}(t), z_{3d}(t))$ is given. For the desired trajectory to be feasible, it must satisfy the equations

$$\begin{aligned} \dot{z}_{1d} &= v_{1d} \\ \dot{z}_{2d} &= v_{2d} \\ \dot{z}_{3d} &= z_{2d}\, v_{1d} \end{aligned}$$

for some choice of the reference inputs $(v_{1d}(t), v_{2d}(t))$. Defining the state errors $e_i = z_{id} - z_i$, for $i = 1, 2, 3$, and the input errors $u_i = v_{id} - v_i$, for $i = 1, 2$, one has the following error dynamics

$$\begin{aligned} \dot{e}_1 &= u_1 \\ \dot{e}_2 &= u_2 \\ \dot{e}_3 &= z_{2d}\, v_{1d} - z_2\, v_1 = v_{1d}\, e_2 + z_{2d}\, u_1 - e_2\, u_1. \end{aligned}$$

Linearization around the reference trajectory yields the time-varying system

$$\dot{\boldsymbol{e}} = \begin{bmatrix} \dot{e}_1 \\ \dot{e}_2 \\ \dot{e}_3 \end{bmatrix} = \begin{bmatrix} 0 & 0 & 0 \\ 0 & 0 & 0 \\ 0 & v_{1d} & 0 \end{bmatrix} \begin{bmatrix} e_1 \\ e_2 \\ e_3 \end{bmatrix} + \begin{bmatrix} 1 & 0 \\ 0 & 1 \\ z_{2d} & 0 \end{bmatrix} \begin{bmatrix} u_1 \\ u_2 \end{bmatrix} = \boldsymbol{A}(t)\boldsymbol{e} + \boldsymbol{B}(t)\boldsymbol{u}.$$

With the linear time-varying feedback

$$\begin{aligned} u_1 &= -k_1\, e_1 \\ u_2 &= -k_2\, e_2 - \frac{k_3}{v_{1d}}\, e_3 \end{aligned}$$

the closed-loop linearized error dynamics becomes

$$\dot{\boldsymbol{e}} = \begin{bmatrix} -k_1 & 0 & 0 \\ 0 & -k_2 & -\frac{k_3}{v_{1d}} \\ -k_1 z_{2d} & v_{1d} & 0 \end{bmatrix} \boldsymbol{e}.$$

The characteristic polynomial of this system is constant:

$$p(\lambda) = (\lambda + k_1)(\lambda^2 + k_2\lambda + k_3).$$

The eigenvalues are thus constant, and have negative real part provided that k_1, k_2 and k_3 are positive. As discussed in Sect. 11.6.1, this does not guarantee stability in view of the time-varying nature of the linearized error dynamics, except for the case when v_{1d} and z_{2d} are constant[1]. In this case, the linearized error system becomes time-invariant, and therefore it is asymptotically stable with the above choice of gains. Hence, the original error system is also asymptotically stable at the origin, although this result is not guaranteed to hold globally.

Solution to Problem 11.15

With reference to the kinematic model (11.19) and Fig. 11.4, consider the following outputs:

$$\begin{aligned} y_1 &= x + \ell\cos\theta + b\cos(\theta+\phi) \\ y_2 &= y + \ell\sin\theta + b\sin(\theta+\phi) \end{aligned}$$

with $b \neq 0$. They represent the Cartesian coordinates of a point P on the line passing through the centre of the front wheel and oriented as the wheel itself, located at a distance $|b|$ from the contact point of the wheel with the ground. The time derivatives of y_1 and y_2 are

$$\begin{aligned} \begin{bmatrix} \dot{y}_1 \\ \dot{y}_2 \end{bmatrix} &= \begin{bmatrix} \cos\theta - \tan\phi(\sin\theta + b\sin(\theta+\phi)/\ell) & -b\sin(\theta+\phi) \\ \sin\theta + \tan\phi(\cos\theta + b\cos(\theta+\phi)/\ell) & b\cos(\theta+\phi) \end{bmatrix} \begin{bmatrix} v \\ \omega \end{bmatrix} \\ &= \boldsymbol{T}(\theta,\phi) \begin{bmatrix} v \\ \omega \end{bmatrix}. \end{aligned}$$

Matrix $\boldsymbol{T}(\theta,\phi)$ has determinant $b/\cos\phi$, and is therefore always invertible under the assumption that $b \neq 0$ and $|\phi(t)| \leq \pi/2$. It is then sufficient to use the following input transformation

$$\begin{bmatrix} v \\ \omega \end{bmatrix} = \boldsymbol{T}^{-1}(\theta,\phi) \begin{bmatrix} u_1 \\ u_2 \end{bmatrix}$$

to put the equations of the bicycle in the input-output linearized form:

$$\begin{aligned} \dot{y}_1 &= u_1 \\ \dot{y}_2 &= u_2 \\ \dot{\theta} &= \sin\phi(\cos(\theta+\phi)u_1 + \sin(\theta+\phi)u_2)/\ell \\ \dot{\phi} &= -(\cos(\theta+\phi)\sin\phi/\ell + \sin(\theta+\phi)/b)u_1 \\ &\quad -(\sin(\theta+\phi)\sin\phi/\ell - \cos(\theta+\phi)/b)u_2. \end{aligned}$$

[1] One may verify that, if the (2,3) chained form represents a unicycle under the transformation (11.23), (11.24), constant values of v_{1d} and z_{2d} correspond to reference trajectories over which ω_d is constant and v_d increases linearly over time (as in an Archimedean spiral).

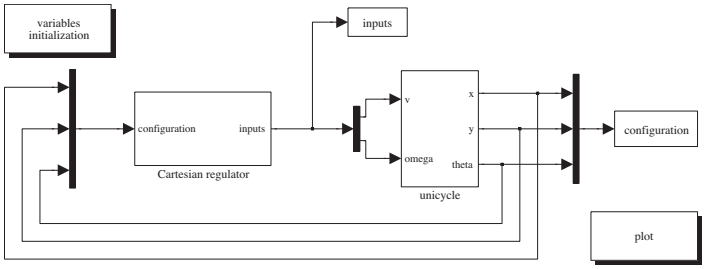

Fig. S11.2. SIMULINK block diagram of the unicycle with the modified cartesian regulator

At this point, a simple linear controller such as

$$u_1 = \dot{y}_{1d} + k_1(y_{1d} - y_1)$$
$$u_2 = \dot{y}_{2d} + k_2(y_{2d} - y_2),$$

with $k_1 > 0$, $k_2 > 0$, guarantees exponential convergence to zero of the Cartesian tracking error, with decoupled dynamics on its two components. Note that the orientation and the steering angle, whose evolutions are governed by the third and fourth equation, are not controlled.

Solution to Problem 11.16

First of all, note that the Cartesian regulator (11.78), (11.79) may be equivalently written as

$$v = k_1 \, \boldsymbol{n}^T \boldsymbol{e}_p \tag{S11.4}$$
$$\omega = k_2 \, \gamma, \tag{S11.5}$$

where $\boldsymbol{n} = [\cos\theta \quad \sin\theta]^T$ is the unit vector aligned with the sagittal axis, $\boldsymbol{e}_p = [-x \quad -y]^T$ is the Cartesian error and $\gamma = \text{Atan2}(y, x) - \theta + \pi$ is the pointing error, i.e., the angle between $\boldsymbol{n}$ and $\boldsymbol{e}_p$ (see also Fig. 11.18). Expression (S11.5) shows that ω induces a rotation until $\boldsymbol{n}$ and $\boldsymbol{e}_p$ align, i.e., until the unicycle points to the origin; as a consequence, the latter will always be reached in forward motion.

Now, redefine the steering velocity (S11.5) as follows:

$$\omega = \begin{cases} k_2 \, \gamma & \text{if } \boldsymbol{n}^T \boldsymbol{e}_p > 0 \\ k_2(\gamma - \text{sign}(\gamma)\pi) & \text{if } \boldsymbol{n}^T \boldsymbol{e}_p \leq 0. \end{cases} \tag{S11.6}$$

With this modification, the unicycle is forced to align with $\boldsymbol{e}_p$ if the pointing error is acute, and with $-\boldsymbol{e}_p$ otherwise. In the second case, the origin will be reached in backward motion.

Unicycle control with the modified position regulator (S11.4), (S11.6) is implemented by the SIMULINK block diagram shown in Fig. S11.2. The files

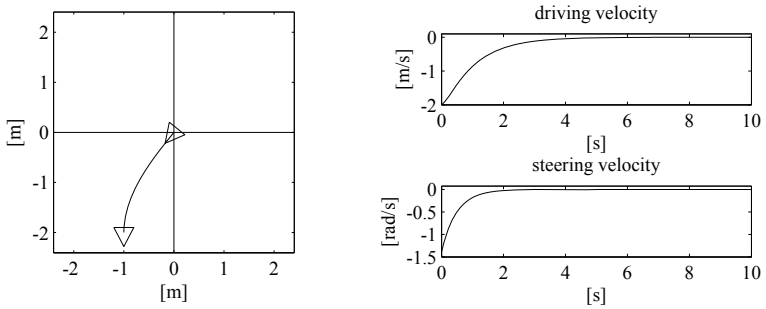

Fig. S11.3. Regulation to the origin of the Cartesian position of the unicycle with the modified controller (S11.4), (S11.6); *left*: Cartesian motion of the unicycle, *right*: time evolution of the velocity inputs v and ω

with the solution can be found in Folder `11_16`. The unicycle is simulated as a continuous-time system using a variable-step integration method, with a maximum step size of 0.01 s. The controller gains can be chosen in the initialization file.

When the initial pointing error is an acute angle, the modified and the original position regulators produce exactly the same trajectories. For example, this is the case of the simulation in Fig. 11.19 (left). However, in the case of Fig. 11.19 (right), the initial pointing error is obtuse, and thus the modified position regulator leads the unicycle to the origin in backward motion, as shown in Fig. S11.3.

Solution to Problem 11.17

Assume that the velocity inputs are constant within each sampling interval:

$$v(t) = v_k \qquad \omega(t) = \omega_k \qquad t \in [t_k, t_{k+1}].$$

Integration of the kinematic equations (11.13) of the unicycle readily provides

$$\theta(t) = \theta_k + \omega_k\,(t - t_k)$$

and

$$\begin{aligned} x(t) &= x_k + v_k \int_0^{t-t_k} \cos\left(\theta_k + \omega_k \tau\right) d\tau = x_k + \frac{v_k}{\omega_k}(\sin\left(\theta_k + \omega_k(t - t_k)\right) - \sin\theta_k) \\ &= x_k + \frac{v_k}{\omega_k}(\sin\theta(t) - \sin\theta_k) \\ y(t) &= y_k + v_k \int_0^{t-t_k} \sin\left(\theta_k + \omega_k \tau\right) d\tau = y_k - \frac{v_k}{\omega_k}(\cos\left(\theta_k + \omega_k(t - t_k)\right) - \cos\theta_k) \\ &= y_k - \frac{v_k}{\omega_k}(\cos\theta(t) - \cos\theta_k). \end{aligned}$$

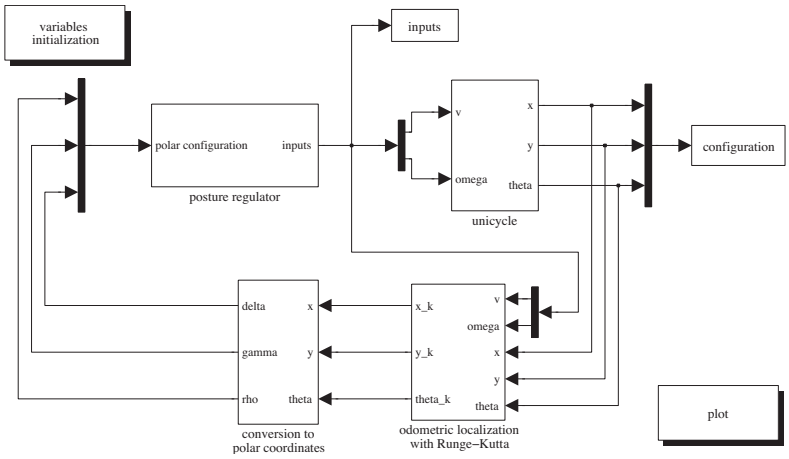

Fig. S11.4. Simulink block diagram of the unicycle with the posture regulator and Runge–Kutta odometric localization

Evaluating the above expressions at $t = t_{k+1} = t_k + T_s$ leads to the odometric prediction (11.85). Alternative proofs can be devised using geometric arguments (the unicycle travels along an arc of circle during each sampling interval) or resorting to a chained-form transformation.

Solution to Problem 11.18

Control of the unicycle with the posture regulator (11.81), (11.82) and Runge–Kutta odometric localization (11.84) is implemented by the SIMULINK block diagram shown in Fig. S11.4. The files with the solution can be found in Folder `11_18`. The unicycle is simulated as a continuous-time system using a variable-step integration method, with a maximum step size of 0.01 s. The controller gains and the duration T_s of the sampling interval for odometric localization can be chosen in the initialization file.

The results obtained with $T_s = 0.01$ s and $T_s = 0.1$ s are shown in Fig. S11.5 and Fig. S11.6, respectively. The initial configuration of the unicycle is the same of Fig. 11.20 (right). Notice how for $T_s = 0.1$ s the low accuracy of the odometric localization does not hinder the convergence of the unicycle to the destination. However, a further increase of T_s will ultimately destabilize the controlled unicycle.

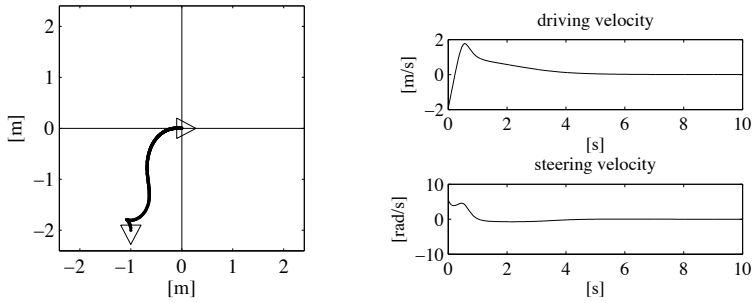

Fig. S11.5. Regulation to the origin of the posture of the unicycle with the controller (11.81), (11.82) and odometric localization (11.84) with $T_s = 0.01$ s; *left*: Cartesian motion of the unicycle (continuous) and odometric estimate (dots), *right*: time evolution of the velocity inputs v and ω

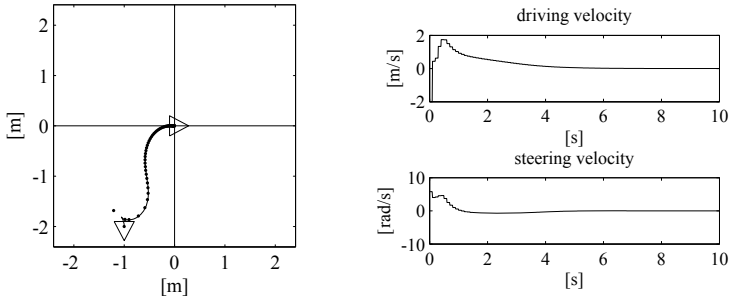

Fig. S11.6. Regulation to the origin of the posture of the unicycle with the controller (11.81), (11.82) and odometric localization (11.84) with $T_s = 0.1$ s; *left*: Cartesian motion of the unicycle (continuous) and odometric estimate (dots), *right*: time evolution of the velocity inputs v and ω